Chapter 9

Parametric Analysis of Electrodeposited Nano-composite Coatings for Abrasive Wear Resistance

Kavian O. Cooke

Additional information is available at the end of the chapter

http://dx.doi.org/10.5772/62153

Abstract

Nano-composite coatings have become the focus of widespread research in recent years due in part to their superior properties when compared to purely metallic films. The benefits of using these types of coatings include high-specific heat, optical non-linearity, novel magnetic properties, enhanced mechanical behavior (large hardness and wear resistance), and good corrosion resistance. This chapter presents a parametric study of electrodeposited nano-composite coatings for improved abrasive wear resistance. The following physical parameters were investigated using a Taguchi L_{18} fractional factorial design of experiments (DOEs): current density, pH, bath temperature, nano-particle concentration, and electrolyte agitation (stir rate). The results were evaluated using the signal-to-noise (S/N) ratio to develop a non-dimensional relationship between the physical parameters and the abrasive wear resistance of the coating. The relationship showed that the abrasive wear resistance of the coating increases as the quantity of nano-particle in the solution and the agitation frequency increase. The analysis of variance (ANOVA) indicated that the particle concentration had the greatest significance to the wear resistance of the coating.

Keywords: Electrodeposition, wear resistance, optimization, Taguchi, nano-composite coating

1. Introduction

Advanced engineering applications often require multifunctional materials with improved performance capabilities, which are usually difficult to fulfill using single-phase materials [1, 2]. The growing demand for improved material performance has led to the development of numerous nano-structured coatings and nano-composite coatings capable of achieving certain technological goals [3–6]. According to Wu et al. [7], these improved properties observed in

nano-coatings have increased their range of application. Currently, these materials find application in medicine, aerospace, automotive, dentistry, electronics, and so on [8–12].

The incorporation of these particles during deposition enables the production of a wide range of composite coatings, which significantly improves the coatings' physical and chemical properties, compared to the pure metallic coatings. These properties are however dependent on the volume of particles that are incorporated in the coating during deposition and the uniformity of the distribution. The amount of incorporated particles is a key parameter for the successful application of the coatings, because it largely determines the properties of composites such as wear resistance, high-temperature corrosion protection, oxidation resistance, and self-lubrication.

The uniformity of the particle distribution within the metal matrix is strongly influenced by the metal matrix morphological and structural characteristics. As such, the co-deposition of a sufficient amount of non-agglomerated particles should lead to production of harder and more wear-resistant coatings. The concentration of particles suspended in solution ranges from 2 g/L up to 200 g/L, producing composites with typically 1–10 vol.% of embedded particles [13].

Particle-reinforced nano-composite coatings based on nickel and alumina are being applied in different technological fields with high demands for wear and corrosion resistance [3]. Lekka et al. [14] show that the co-deposition of SiC nano-particles in copper matrix leads to a more noticeable grain refinement, and therefore, the nano-composite deposits presented a very high micro-hardness, 61% higher than pure copper deposits, and an increase of 58% of the abrasion resistance. Future applications of these materials depend on the ability to produce them with controlled composition and properties, using inexpensive and reliable techniques.

Electrodeposition method satisfies some of these requirements because it is an economical and versatile technique compared to other preparation techniques. Electrodeposited nano-composite coatings are generally obtained by suspending charged ceramic nano-particles in the electrolyte and co-depositing them with the metal. During the electrodeposition process, these insoluble hard particles are suspended in a conventional plating electrolyte and are captured in the growing metal film during deposition. An effective dispersion of inert particles in the electrolyte promotes the adsorption opportunity of inert particles on the cathode and causes a higher volume content of inert particles in the composite coating. The mechanical properties of the composite coating are also promoted by the enhancement of the volume content of inert particles in the coating [15–17].

Two mechanisms have been proposed to describe the process by which ceramic particles are incorporated in the metallic coatings: (1) the first mechanism is known as electrophoresis. The electrophoresis process begins with particles that are well dispersed and are able to move independently in the solvent suspension, and the particles have a surface charge due to electrochemical equilibrium with the solvent. This leads to a migratory attraction of the particles to the deposition electrode [18]. (2) A second mechanism was proposed by Williams and Martin in 1964. In their study, the researchers suggested that the particles were transported to the cathode by a purely mechanical mean due to the agitation of the bath, which leads to entrapment and subsequent embedding of the particles in the growing metal layer [19].

http://dx.doi.org/10.5772/62153

However, the validity of mechanical particle entrapment theory was later challenged by Brandes and Goldthorpe, who suggested that there is some attractive force holding the particles at the cathode long enough to be incorporated by the growing metal layer [20]. Guglielmi proposed a two-step mechanism taking into account electrophoresis and adsorption.

In the first step, particles approaching the cathode become loosely adsorbed on the cathode surface [21]. These loosely adsorbed particles are still surrounded by a cloud of adsorbed ions. In the second step, the particles lose this ionic cloud and become strongly adsorbed on the cathode. This step is thought to be of an electrochemical character; that is, it depends on the electrical field at the cathode. Finally, the strongly absorbed particles are occluded by the growing metal layer [1, 22–25]. One method that has been used to reduce particle coagulation is mechanical stirring [26]. If a particle is strongly adsorbed on the cathode, it will be embedded on the growing metal layer by the electrodeposition of free solvated electro-active ions from the plating bath [3, 23].

According to the scientific literature, the factors that affect the coating properties are directly related to the parameter settings during the deposition process, and as such optimization is an important step in coating development. This chapter presents a parametric study of electrodeposited nano-composite coatings for improved abrasive wear resistance using the Taguchi L_{18} design of experiments (DOEs). The main focus is to evaluate the effects of the coating parameters on its wear resistance, with the objectives being to identify the optimal setting of each parameter and to quantify the contribution of each parameter to the wear resistance of the coating.

2. Experimental Procedure

2.1. Parametric design using Taguchi techniques

In this study, parametric optimization was achieved using Taguchi L_{18} fractional factorial DOE to evaluate the parameters of the electroplating process used for depositing the Ni/Al_2O_3 composite coating for improved hardness and wear resistance. The main process parameters evaluated were cathode current density and agitation/stir rate (A), the pH level of the solution (B), particle concentration (C), and bath temperature (D). The parameter settings used, shown in Table 1, were determined through preliminary investigation and represent three different level settings (levels 1–3). The orthogonal array is presented in Table 2 and shows the parameter combination for each of the 18 experimental runs using the level settings, as shown in Table 1 [27].

The optimization can be achieved by calculating the signal-to-noise (S/N) ratio as a quality tool for evaluating the performance of the coatings produced. The S/N ratio (η) represents the degree of predictable performance of the coatings in the presence of noise factors. To calculate the S/N ratio, the average and variation of the experimental results can be determined using Equation 1 [6].

$$\eta = -10 \log(\text{MSD}), \tag{1}$$

where MSD is the mean square deviation for the output characteristic. As the aim of this study is to minimize the wear loss of the coating, the smaller-is-better quality characteristic was selected and can be calculated using Equation 2 [28].

$$\text{Smaller is better} - \text{MSD} = \frac{1}{n}\sum_{i=1}^{n} y_i^2 \tag{2}$$

Level	Current density (A/mm^2)	Stir rate (rpm) (A)	Bath pH (B)	Al_2O_3 concentration (g/L) (C)	Bath temperature (°C) (D)
1	2.3	440	4.0	10	40
2	2.5	600	4.45	20	50
3	–	800	4.6	30	60

Table 1. Experimental levels used for electrodeposition process.

Experiment	Controlled parameters				
	A	B	C	D	E
1	1	1	1	1	1
2	1	1	2	2	2
3	1	1	3	3	3
4	1	2	1	1	2
5	1	2	2	2	3
6	1	2	3	3	1
7	1	3	1	2	1
8	1	3	2	3	2
9	1	3	3	1	3
10	2	1	1	3	3
11	2	1	2	1	1
12	2	1	3	2	2
13	2	2	1	2	3
14	2	2	2	3	1
15	2	2	3	1	2
16	2	3	1	3	2
17	2	3	2	1	3
18	2	3	3	2	1

Table 2. Taguchi L_{18} orthogonal array.

http://dx.doi.org/10.5772/62153

On the other hand, given the relationship between hardness and wear resistance [3], the larger-the-better characteristic was used to optimize the coating for hardness, as shown in Equation 3:

$$\text{Larger is better} - \text{MSD} = \frac{1}{n}\sum_{i=1}^{n}\frac{1}{y_i^2}, \tag{3}$$

where y_i is the value of wear resistance for the ith test; and n is the number of tests.

The average value of the response variable at each parameter level was determined by applying Equation 4 to each parameter level for each factor [24]:

$$m_{A1} = \frac{1}{3}(\eta_1 + \eta_2 + \eta_3). \tag{4}$$

2.2. ANOVA

The analysis of variance (ANOVA) was carried out to examine the influence of each process parameter on quality characteristics. If some parameters do not significantly affect wear rate, they can be fixed to a minimum level and excluded from the optimization process. The percent contribution of each parameter was calculated by determining the total sum of squared deviation and the individual contribution of each parameter to the sum of squared deviations. These variables were calculated using Equations 7:

$$\text{SS}_\text{T} = \frac{1}{n}\sum_{i=1}^{9}(\eta_i - \bar{\eta})^2 \tag{5}$$

$$\bar{\eta} = \frac{1}{9}\sum_{i=1}^{9}\eta_i \tag{6}$$

$$\text{SS}_\text{d} = 3x(\eta_{A1} - \bar{\eta})^2 + 3x(\eta_{A2} - \bar{\eta})^2 + 3x(\eta_{A3} - \bar{\eta})^2 \tag{7}$$

The percentage contribution (ρ) of each factor to the overall response is determined using Equation 8:

$$\rho = \frac{\text{SS}_\text{d}}{\text{SS}_\text{T}} \times 100. \tag{8}$$

2.3. Sample preparation and characterization

The mild steel samples of dimensions 0 × 20 × 15 mm were cut, prepared to 800-grit abrasive paper, and polished to 1-μm diamond suspension, after which they were cleaned in an acetone bath (see Figure 1a). Acid pickling took place in a solution of 15 wt.% HNO_3 and 2 wt.% HF at 50°C for 2 minutes and then rinsed in distilled water. These samples were then used as the cathode in the plating solution.

The electrodeposition of an Ni/Al_2O_3 coating was carried out in a 250-mL glass beaker, as shown in Figure 1(b). The plating solution was prepared by dissolving 250 g/L $NiSO_4$ $6H_2O$, 45 g/L $NiCl_2$ $6H_2O$, 35 g/L H_3BO_3, and 1 g/L saccharin in distilled water. The ceramic particles were added separately to the nickel bath to produce the composite coating. The particles were thoroughly mixed into the solution for 2 hours and kept in suspension in the bath with a magnetic stirrer. The following parameters were adjusted: cathode current density, agitation, and stir rate (A); the pH level of the solution (B); concentration of composite particles (C); and bath temperature (D), as shown in Table 1. The thickness of Ni/Al_2O_3p coatings was controlled by the plating time. The actual amount of Ni/Al_2O_3p electroplated onto a surface was determined by the weight gain after the plating process.

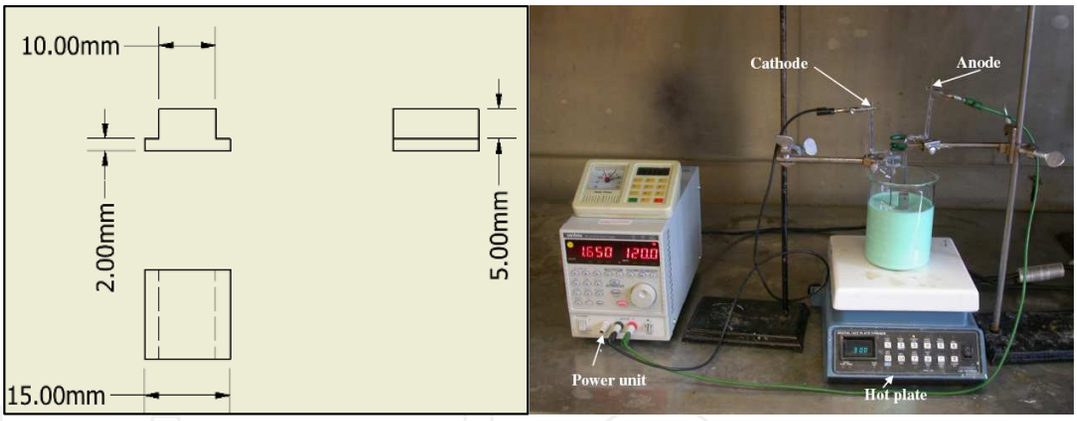

Figure 1. (a) Specimen size of wear resistance test sample and (b) electroplating equipment and setup.

Coated samples were evaluated for hardness using a Vickers Mitutoyo HM-122 hardness tester with a load of 200 g. Two body abrasive wear tests were conducted using Plint Multi-station Block-on-Ring tester under a load of 20 N at a fixed sliding speed of 3.35 m/s for a sliding distance of 5000 m against steel disc of hardness 500 HV. During sliding, the load is applied on the specimen through cantilever mechanism, and the specimens brought in intimate contact with the rotating disc at a track radius of 100 mm. The samples were cleaned with acetone and weighed (up to an accuracy of 0.01 mg using a Sartorius microbalance) before and after each test. The wear rate was calculated from the weight loss measurement and expressed in terms of volume loss per unit sliding distance.

http://dx.doi.org/10.5772/62153

For each coated sample, three specimens were tested and the average value was used to determine the wear resistance. Examination of the joints microstructure was performed using a Ziess optical microscope, an ASPEX 309 scanning electron microscope (SEM), and a transmission electron microscope (TEM). Quantitative compositional analyses were carried out using wavelength dispersive spectroscopy (WDS) and x-ray diffraction (XRD). Micro-hardness testing was performed on the cross section of the joints according to ASTM E92 standard test method for a Vickers micro-hardness testing. Indentations were made at 100 μm spacing using a diamond tip indenter to which a 0.2 kg load was applied for 15 seconds, after which the length of the diagonals was measured and the hardness number was recorded from tables.

For TEM analyses, sections of the coating were cut to 6 × 5 × 1.5 mm using a thin diamond tip cutter and subsequently mechanically grounded using 600 grit abrasive paper to a thickness of approximately 200 μm. Disc of 3 mm diameter was punched from the 200-μm coating and subsequently mechanically grinded to 25 μm. The grinded samples were thinned by electropolishing method. This was done in a solution containing 150 g/L Na_2CO_3 + 50 g/L Na_3PO_4 + 30 g/L. The solution was maintained at a temperature of 40°C and a voltage of 20 V. All the thinned coatings were examined with a JEOL TEM 2000FX TEM at an accelerating voltage of 200 kV.

3. Results and Discussion

3.1. Microstructure analysis

The TEM micrograph of the Ni/Al_2O_3 coating, as shown in Figure 2(a), revealed the presence of nanosized Al_2O_3 particles embedded in the nickel matrix. The deposition of particle reinforcement during the coating process can be attributed to parameters such as current densities, bath temperature, stir rate, bath pH, and particle concentration [29]. TEM analysis of the as-received powder shown in Figure 2(b) indicated the presence of agglomerated particle clusters. These particle clusters are believed to have been subsequently embedded in the coating during the electrodeposition process. In situations where particle clustering is present, surfactants such as saccharin, hexadecylpyridinium bromide (HPB), and cetyltrimethylammonium bromide (CTAB) are used to improve particle distribution and reduce clustering [4, 30, 31]. In this study, the surfactant saccharin was used to reduce particle clustering; however, particle agglomeration was still present, as shown in Figure 2(a).

An optical micrograph of the nano-composite Ni/Al_2O_3 coating deposited using current density 3.2 × 10^{-4} A/mm^2, stir rate 440 rpm, bath temperature 50°C, pH 4.45, and particle concentration 20 g/L is shown in Figure 3(a). Analysis of the image revealed Al_2O_3 particle clusters consistent with the particle agglomeration observed in the as-received Al_2O_3 powder is shown in Figure 3(b). Similar surface morphology obtained for coatings deposited using current density 5 × 10^{-4}A/mm^2, stir rate 820 rpm, bath temperature 60°C, pH 4.45, and particle concentration 10 g/L was observed to posses large globules that are believed to be agglomerated Al_2O_3 particles embedded into the Ni matrix.

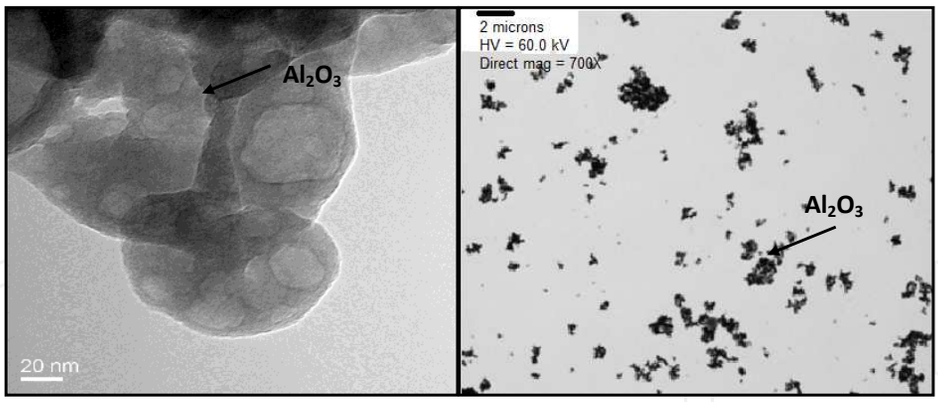

Figure 2. TEM image of the Ni/Al_2O_3coating.

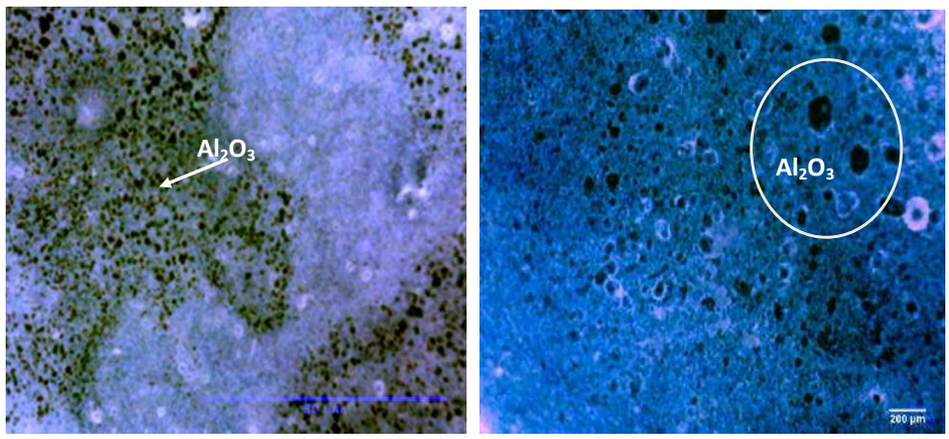

(a) (b)

Figure 3. Optical micrograph of coatings deposited with the parameters outlined in experiment: (a) 2 and (b) 17, as shown in Table 2.

3.2. Micro-hardness

The influence of the process parameters was assessed to maximize the coating hardness. Analysis of the surface hardness revealed that if the parameters were set to current density at level 1 (3.2×10^{-4} A/mm^2), revolutions per minute (RPM) at level 2 (630 rpm), pH at level 2 (4.45), Al_2O_3 concentration at level 3 (30 g/L), and temperature at level 2 (50°C), a surface hardness of 501.5 HV can be achieved. When compared with pure nickel, a surface hardness of 278.82 HV was achieved. The differences observed were attributed to dispersion hardening effects caused by the presence of nanosized Al_2O_3 in the composite coating. According to Lehman et al. [32], the nanosized particles act to restrict/reduce dislocation motion in the nickel matrix, which causes an increase in the surface hardness. The ANOVA test showed that stir rate (RPM), particle concentration, and bath pH had the greatest impact on the hardness of the coatings.

http://dx.doi.org/10.5772/62153

Stir rate (RPM) is used to disperse the nano-particles during the coating process, thus controlling the microstructure produced by keeping particles suspended in the bath solution during coating [33, 34]. It is believed that stirring increases the amount of nano-particles embedded in the coating up to 630 rpm beyond which a reduction in surface hardness is observed.

Similar effects were observed when the concentration of Al_2O_3 particles suspended in the solution increased. The results indicated that particle incorporated into the coating increased with increasing particle concentration in the bath solution until 30 g/L was reached. The microstructure of the coating may also be attributed to the pH of the bath which is believed to control the nucleation and morphology of the coating; as the pH decreases, the grain size of the crystallite also decreases, resulting in an increase in the hardness of the material [35, 36]. The estimated effect of each parameter is shown graphically in Figure 4. Analysis of the data using the larger-is-better characteristics indicated that optimum coating hardness can be achieved if concentration is set to level 3, while all other parameters are set to level 2.

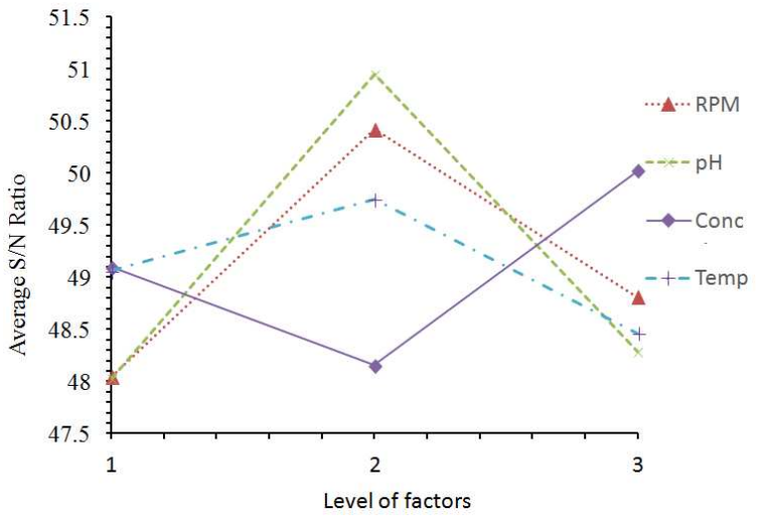

Figure 4. Effect of process parameters on micro-hardness.

3.3. Wear testing

Two-body abrasive wear tests were carried out to evaluate the effects of electroplating parameters on the wear resistance of the deposited coating. Evaluation of the results presented in Table 3 indicated that the wear rate increased from 0.22 kg/s to 2.11 kg/s. The estimated effect of each parameter is shown graphically in Figure 5. Analysis of the data using the smaller-is-better characteristics indicated that the S/N ratio decreased as the stir rate increased from 440 rpm to 630 rpm; however, increasing the stir rate to 820 rpm corresponded to an increase of the S/N ratio; this change can be attributed to achieving suitable particle suspension in the solution at 630 rpm; however, further increase in stir rate caused an increase turbulence in the solution, which can reduce particulate inclusion in the Ni matrix [34]. The impact of bath pH and temperature had similar effects on the S/N ratio [34]. The results indicated that minimal mass loss can be achieved if both pH and temperature are set to level 1 [37].

In addition, the results further revealed that particle concentration had a significant effect on the wear rate, which corresponded to an increase in the hardness of the coatings deposited as the particle concentration increased from 10 g/L to 20 g/L. The reduction in wear rate was attributed to the increase in the Al_2O_3 particles embedded in the Ni matrix during the co-deposition process. The Al_2O_3 nano-particulates co-deposited in the Ni matrix could restrain the Ni grains and the plastic deformation of the matrix under a loading due to dispersion strengthening. The effect is that the coating becomes stronger as the nano-Al_2O_3 particle content increases, thus increasing micro-hardness and wear resistance of the coating. Further increase in the particle content resulted in increase of the brittleness of the coating, which is subsequently reflected as a reduction of the wear resistance of the coating. By utilizing the wear resistance values shown in Table 4, the optimum coating parameters were determined to be A2, B1, C2, and D1.

Experiment	Current density (A/mm²; × 10⁻⁴)	Stir rate (A) (rpm)	pH (B)	Concentration (C) (g/L)	Temperature (D) (°C)	Hardness (HV)	S/N (η; dB)	Wear rate (×10⁻⁶) (kg/s)	S/N (η; dB)
1	3.2	440	4.3	10	40	208.5	46.38	2.11	116.32
2	3.2	440	4.45	20	50	318.3	50.06	1.00	122.50
3	3.2	440	4.6	30	60	268.3	48.57	0.220	137.44
4	3.2	630	4.3	10	50	357.3	51.06	0.44	131.19
5	3.2	630	4.45	20	60	325.5	50.25	1.10	122.59
6	3.2	630	4.6	30	40	369.4	51.35	0.88	124.32
7	3.2	820	4.3	20	40	300	49.54	0.66	128.05
8	3.2	820	4.45	30	50	363.9	51.22	0.55	129.39
9	3.2	820	4.6	10	60	199.9	46.02	1.00	123.36
10	5	440	4.3	30	60	224.5	47.02	0.66	127.16
11	5	440	4.45	10	40	282.1	49.01	0.33	133.18
12	5	440	4.6	20	50	229.9	47.23	0.55	128.36
13	5	630	4.3	20	60	219	46.81	1.00	122.84
14	5	630	4.45	30	40	449.8	53.06	0.22	136.57
15	5	630	4.6	10	50	582.9	49.99	1.00	122.18
16	5	820	4.3	30	50	279.7	48.93	0.33	133.18
17	5	820	4.45	10	60	403.5	52.12	0.33	132.38
18	5	820	4.6	20	40	178.5	45.03	0.88	124.22

Table 3. Measured results of response variables and S/N ratios.

http://dx.doi.org/10.5772/62153

Factors	Code	Wear rate S/N ratio (dB)			Hardness S/N ratio (dB)		
		1	2	3	1	2	3
Stir rate	A	127.49	126.6	128.43	48.05	50.42	48.81
pH level	B	126.46	129.43	126.65	48.03	50.95	48.29
Al_2O_3 concentration	C	126.44	124.76	131.34	49.1	48.15	50.03
Bath temperature	D	128.47	130.76	129.30	49.06	49.75	48.46

Table 4. Mean S/N ratio of individual levels.

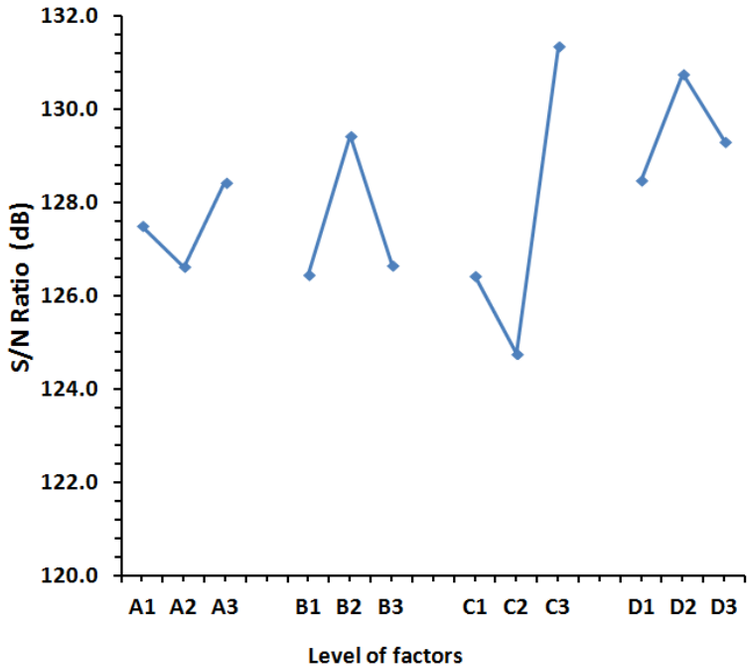

Figure 5. Effect of process parameters on wear resistance.

3.4. Analysis of the level averages

A second analysis using the level averaging technique was also carried out by averaging the experimental results achieved at each level for the respective parameter. A summary of these calculations is shown in Table 5 and is graphically represented in Figure 6. When the effects of stir rate and concentration were evaluated, it was found that the wear rate decreased as both concentration and stir rate increased similar to the results obtained when the S/N ratio was calculated. The optimum wear resistance can be obtained by setting both the stir rate and concentration are set to level 3, whereas bath temperature and pH are set to level 2. Optimization for hardness revealed that all the parameter settings were similar with the only exception being stir rate, which required a level 2 setting (Figure 7). These results are also consistent with literature [34, 37].

Factors	Code	Parameter levels(wear resistance test) × 10^{-7}			Hardness $HV_{0.2\,kg}$		
		1	2	3	1	2	3
Current density		8.84	5.89	0	301.2	287	0
RPM	A	8.12	7.73	6.25	255.3	339.5	287.6
pH	B	7.55	5.88	8.67	260.3	306.2	264.8
Al_2O_3 concentration	C	8.68	8.65	4.77	294.5	261.9	325.9
Bath temperature	D	8.47	6.45	7.18	298.1	310.8	273.5

Table 5. Level averages for each parameter.

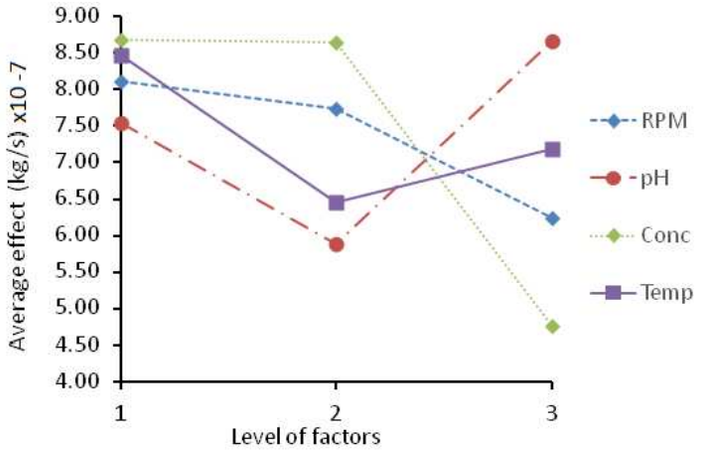

Figure 6. Mean wear rate of each parameter level.

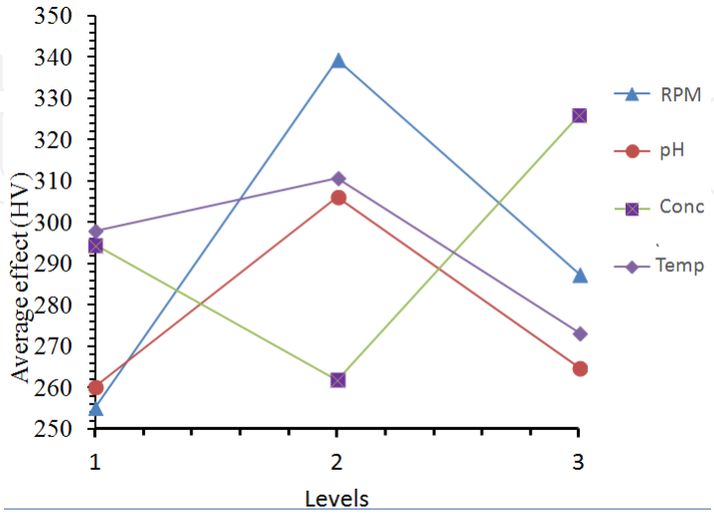

Figure 7. Mean hardness of each parameter level.

http://dx.doi.org/10.5772/62153

3.5. ANOVA

The ANOVA separates the total variability of the response into percentage contribution (P) of each parameter. The higher the percentage contribution, the more important the parameter is to the wear resistance and hardness of the coating. Table 6 shows the ANOVA calculated values and indicates that the greatest contributing factor for wear was the Al_2O_3 particle concentration at 51.68% followed by bath temperature with a contribution of 32.41%, whereas bath pH and stir rate had the lowest impact on the wear resistance of the coating.

Factors	Code	DOF	Sum of squares	Variance	Contribution(%)
Stir rate	A	2.00	5.0	2.48	3.64
pH	B	2.00	16.67	8.33	12.27
Al_2O_3 concentration	C	2.00	70.20	35.10	51.68
Bath t**emperature**	D	2.00	44.03	22.01	32.41
Total		8.00	135.8		100.0

Table 6. ANOVA for wear.

3.6. Selection of the optimum parameters

To select the optimum parameter settings for improved wear resistance, the "smaller-is-better" characteristics were used to select the optimized parameter level, which are shown in Table 7. Table 7 indicates one conflict in the recommended optimized levels: factor A (stir rate). Analysis of the results for both S/N ratio averages and the level averages revealed that the stir rate greater than 630 rpm would result in minimum output; however, analysis of the level-averaged wear rate indicated that a setting at level 2 would be more appropriate. The results suggest that within the parameter levels tested, pH and stir rate had the least effect on the wear rate.

Factors	Code	Optimized levels	
		$\bar{Y}$	S/N ratio
Stir rate	A	3	2
pH	B	2	2
Al_2O_3 concentration	C	3	3
Bath temperature	D	2	2

Table 7. Summary of the factor analysis.

3.7. Confirmation test

Experimental validation of the Taguchi optimization process was necessary to confirm that the minimum wear rate can be achieved using the optimum coating parameters. A conforma-

tional experiment was conducted with the levels of the process parameters (A3, B2, C3, and D2), resulting from the optimization process. Two wear rate values were obtained (4.4E-07 kg/s and 4.1E-07 kg/s), and the average of these values was found to be 4.25E-07 kg/s with an average hardness of 501.5 HV.

An SEM micrograph of the optimized Ni/Al_2O_3 coating as shown in Figure 8(a) revealed the absence of surface defects and interfacial voids; however, agglomerate Al_2O_3 particles were present in the coating.

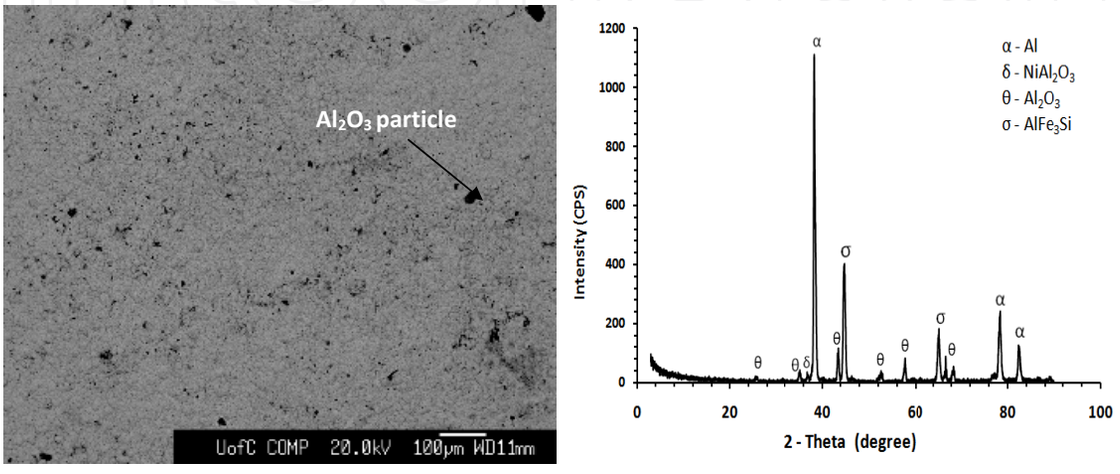

(a) (b)

Figure 8. (a) Surface of Ni/Al_2O_3 coating and (b) XRD spectrum of coated samples.

4. Conclusion

In this chapter, the recent development in the production and utilization of electrodeposited nano-composite coatings was examined. It was found that the tribological application of nano-composite coatings was strongly dependent on their compositional, morphological, and structural characteristics. According to the literature, these properties are directly related to the preparation method and deposition conditions such as current density, substrate, pH, ion concentration, size and quantity of nano-particles, and agitation frequency. Thus, the optimization of the parametric setting is of critical importance to assess the wear resistance of the coating.

The results demonstrated that Taguchi DOEs can be effectively used to optimize the electrodeposition process; however, due to material limitations the experiment was restricted to the use of only two samples per condition. Increasing the temperature and particle concentration caused a reduction in the wear rate of the coating. The results also show that increasing temperature to 50°C caused a reduction in the wear rate of the coatings deposited. Stir rate is the parameter having the least effect on the wear rate of the coatings.

The combination of optimum bonding parameters within the experimental level ranges is found to be a temperature of 50°C, particle concentration 30 vol.%, stir rate 820 rpm, and pH 4.45. Within the experimental level ranges, the most significant influencing parameter is particle concentration, which accounts for 51.68% of the total effect, followed by temperature (32.41), bath pH, and stir rate (12.27% and 3.64%, respectively).

Author details

Kavian O. Cooke

Address all correspondence to: kavian_cooke@yahoo.com

Department of Mechanical Engineering, University of Technology, Jamaica, Kingston, Jamaica

References

[1] Cao, G. Nanostructures and Nanomaterials – Synthesis, Properties and Applications.Published by Imperial College Press, United Kingdom, 2004.

[2] Low, C.T.J. and Walsh, F.C. Self-lubricating metal composite coatings by electrodeposition or electroless deposition. Encyclopedia of Tribology, 3025–3031, ISBN: 978-0-387-92896-8, 2013.

[3] Jung, A., Natter, H., Hempelmann, R. and Lach, E. Nanocrystalline alumina dispersed in nanocrystalline nickel: Enhanced mechanical properties. Journal of Materials Science, 44, 2725–2735, 2009.

[4] Chen, L., Wang, L., Zeng, Z. and Zhang, J. Effect of surfactant on the electrodeposition and wear resistance of Ni–Al_2O_3 composite coatings. Materials Science and Engineering A, 434, 319–325, 2006.

[5] Sheng-Lung, K. Effect of nickel ion concentration on Ni/Al_2O_3 composite coatings. Journal of the Chinese Institute of Engineers, 28(1), 1–8, 2005.

[6] Parida, G., Chaira, D., Chopkar, M. and Basu, A. Synthesis and characterization of Ni–TiO_2 composite coatings by electro-co-deposition, 205 issues 21-22, 4871-4879, 2011.

[7] Wu, G., Li, N., Zhou, D.R. and Mitsuo, K. Electrodeposited Co–Ni–Al_2O_3 composite coatings. Journal of Surface and Coatings Technology, 176, 157−164, 2004.

[8] Moritz, T., Eiselt, W. and Moritz, K. Electrophoretic deposition applied to ceramic dental crowns and bridges. Journal of Materials Science, 41, 8123–8129, 2006.

[9] Hou, K.H., Ger, M.D., Wang, L.M. and Ke, S.T. The wear behaviour of electro-codeposited Ni/SiC composites. Wear, 253, 994–1003, 2002.

[10] Garcia, I., Fransaer, J. and Celis, J.-P. Electrodeposition and sliding wear resistance of nickel composite coatings containing micron and submicron SiC particles. Surface and Coatings Technology, 148, 171–178, 2001.

[11] Bicelli, L.P., Bozzini, B., Mele, C. and D'Urzo, L. A review of nanostructural aspects of metal electrodeposition. International Journal of Electrochemical Science, 3, 356–408, 2008.

[12] Rusu, D.E., Cojocaru, P., Magagnin, L., Gheorghies, C. and Carac, G. Study of Ni–TiO_2 nanocomposite coating prepared by electrochemical deposition. Journal of Optoelectronics and Advanced Materials, 12(12), 2419–2422, 2010.

[13] Stojak, J.L., Fransaer, J. and Talbot, J.B. Review of Electrocodeposition. In Alkire, R.C. and Kolb, D.M. (Eds.), Advances in Electrochemical Science and Engineering, Vol. 7, John Wiley and Sons-VCH Verlag, Germany, 5-30, ISBN: 3-527-29830-4, 2002.

[14] Lekka, M., Koumoulis, D., Kouloumbi, N. and Bonora, P.L. Mechanical and anticorrosive properties of copper matrix micro- and nano-composite coatings. Electrochimica Acta, 54, 2540–2546, 2009.

[15] Foster, J. and Cameron, B. Effect of current density and agitation on the formation of electrodeposited composite coatings. Transactions of the Institute of Metal Finishing, 54(4), 178–183, 1976.

[16] Shao, I., Vereecken, P.M., Cammarata, R.R. and Searson, P.C. Kinetics of particle code-position of nanocomposites. Journal of the Electrochemical Society, 149(11), 610-614, 2002.

[17] Benea, L., Bonora, P.L., Borello, A., Martelli, S., Wenger, F., Ponthiaux, P. and Galland, J. Composite electrodeposition to obtain nanostructured coatings. Journal of the Electrochemical Society, 148(7), C461–C465, 2001.

[18] Whithers, J.C. Electrochemical co-deposition by electrophoresis, Production Finhing. 26, 62, 1962.

[19] Williams, R.V. and Martin, P. W. Electrodeposition and metal finishing, Transactions of the Institute of Metal Finishing, 42, 182, 1964.

[20] Brandes, E.A. and Goldthorpe, Electrodeposition of cermets, D. Metallurgia 76, 195, 1967.

[21] Guglielmi, N. Kinetics of the deposition of inert particles from electrolytic baths. Journal of Electrochemistry Society, 119(8), 1009–1012, 1972.

[22] Gomes, A., Pereira, I., Fernández, B. and Pereiro, R. Electrodeposition of Metal Matrix Nanocomposites: Improvement of the Chemical Characterization Techniques. Intech Open, Croatia, 21–46.

[23] Hunter, R.J. Zeta Potential in Colloids Science. Academic Press, New York, 1981.

[24] Boccaccini, A.R. and Zhitomirsky, I. Application of electrophoretic and electrolytic deposition techniques in ceramics processing. Current Opinion in Solid State and Materials Science, 6, 251–260, 2002.

[25] Kunio, F. and Hideo, M. Dekker Encyclopedia of Nanoscience and Nanotechnology, Editor Cristian Contecu. In Colloidal Nanoparticles: Electrokinetic Characterization, 2nd ed.United States, 773–785, 2009.

[26] Fransier, J., Celis, J.P. and Roos, J.R.Electrochemical preparation of oxide-matrix composites Journal of Electrochemistry Society, 141, 669, 1994.

[27] Belavendram, N. Design by Quality – Taguchi Techniques for Industrial Experimentation. Prentice Hall, London, 1995.

[28] Dobrzañski, L.A., Domaga, J. and Silva, J.F. Application of Taguchi method in the optimization of filament winding of thermoplastic composites.Archives of Material Science and Engineering 28(3), 133–140, 2007.

[29] Goral, A., Beltowska-Lehman, E. and Indyka, P. Structure characterization of Ni/Al_2O_3 composite coatings prepared by electrodeposition. Solid State Phenomena, 163, 64–67, 2010.

[30] Aruna, S.T., Selvi, V.E., Grips, W.V. and Rajam, K.S. Corrosion and wear resistant properties of Ni-Al_2O_3 composite coatings containing various forms of alumina. Journal of Applied Electrochemistry, 41, 461–468, 2011.

[31] Badarulzaman, N.A., Purwadaria, S., Mohamad, A.A. and Ahmad, Z.A. The production of nickel–alumina composite coating via electroplating. Ionics: The International Journal of Ionics: The Science of Technology and Ionic Motion, 15, 603–607, 2009.

[32] Beltowska Lehman, E., Goral, A. and Indyka, P. An electrodeposition and characterization of Ni/Al_2O_3 nanocomposite coatings. Achives of Metallurgy and Materials, 56(4), 919-931, 2011. DOI:10.2478/v10172-011-0101-1.

[33] Ahmad, Y. and Mohamed, A.M. Electrodeposition of nanostructured nickel-ceramic composite coatings: A review. International Journal of Electrochemical Science, 9, 1942–1963, 2014.

[34] Rostami, M., Saatchi, A. and Ebrahimi-Kahrizsangi, R. Influences of bath stiring rate on synetics of nano composite NiSiCGr coatings on St37 via electrodeposition process. Journal of Advanced Materials and Processing, I, 11–19, 2013.

[35] Aruna, S.T., Diwakar, S., Jain, A. and Rajam, K.S. Comparative study on the effect of current density on Ni and Ni–Al_2O_3 nanocomposite coatings produced by electrolytic deposition. Surface Engineering, 21, 209–214, 2005.

[36] Lu, W., Ou, C., Huang, P., Yan, P. and Yan, B. Effect of pH on the structural properties of electrodeposited nanocrystalline FeCo films. International Journal of Electrochemical Sciences, 8218–8226, 2013.

[37] Gopalsamy, B., Mondal, B. and Ghosh, S. Taguchi method and ANOVA: An approach for the process parameters optimization of hard machining while machining hardened steel. Journal of Scientific and Industrial Research, 68, 686–695, 2009.

IntechOpen